

NeuroXplorer 1.0: An Extensible Framework for Architectural Exploration with Spiking Neural Networks

Adarsha Balaji
ab3586@drexel.edu
Drexel University
Philadelphia, PA, USA

Shihao Song
ss3695@drexel.edu
Drexel University
Philadelphia, PA, USA

Twisha Titirsha
tt624@drexel.edu
Drexel University
Philadelphia, PA, USA

Anup Das
anup.das@drexel.edu
Drexel University
Philadelphia, PA, USA

Jeffrey L. Krichmar
jkrichma@uci.edu
University of California, Irvine
Irvine, CA, USA

Nikil Dutt
dutt@ics.uci.edu
University of California, Irvine
Irvine, CA, USA

James Shackleford
jas64@drexel.edu
Drexel University
Philadelphia, PA, USA

Nagarajan Kandasamy
nk78@drexel.edu
Drexel University
Philadelphia, PA, USA

Francky Catthoor
Francky.Catthoor@imec.be
Imec
Leuven, Belgium

ABSTRACT

Recently, both industry and academia have proposed many different neuromorphic architectures to execute applications that are designed with Spiking Neural Network (SNN). Consequently, there is a growing need for an extensible simulation framework that can perform architectural explorations with SNNs, including both platform-based design of today's hardware, and hardware-software co-design and design-technology co-optimization of the future. We present NeuroXplorer, a fast and extensible framework that is based on a generalized template for modeling a neuromorphic architecture that can be infused with the specific details of a given hardware and/or technology. NeuroXplorer can perform both low-level cycle-accurate architectural simulations and high-level analysis with data-flow abstractions. NeuroXplorer's optimization engine can incorporate hardware-oriented metrics such as energy, throughput, and latency, as well as SNN-oriented metrics such as inter-spike interval distortion and spike disorder, which directly impact SNN performance. We demonstrate the architectural exploration capabilities of NeuroXplorer through case studies with many state-of-the-art machine learning models.

CCS CONCEPTS

• **Hardware** → **Neural systems; Emerging languages and compilers; Emerging tools and methodologies.**

KEYWORDS

Spiking Neural Networks (SNN), Neuromorphic Computing, Non Volatile Memory (NVM), Platform-Based Design, Hardware-Software Co-Design, Design-Technology Co-Optimization

ACM Reference Format:

Adarsha Balaji, Shihao Song, Twisha Titirsha, Anup Das, Jeffrey L. Krichmar, Nikil Dutt, James Shackleford, Nagarajan Kandasamy, and Francky Catthoor. 2021. NeuroXplorer 1.0: An Extensible Framework for Architectural Exploration with Spiking Neural Networks. In *ICONS '21: ACM International Conference on Neuromorphic Systems, June 03–05, 2018, Virtual Conference*. ACM, New York, NY, USA, 9 pages. <https://doi.org/10.1145/1122445.1122456>

1 INTRODUCTION

The term neuromorphic computing was coined in the 90s to describe integrated circuits that mimic the neuro-biological architecture of the central nervous system [42]. These circuits employ variants of integrate-and-fire (I&F) neurons [28] as computational units and analog weights as synaptic storage. I&F neurons use spikes to encode information, where each spike is a voltage or current pulse in the physical world, typically of ms duration [40]. Recently, both industry and academia have proposed many different neuromorphic platforms to execute applications that are designed with Spiking Neural Network (SNN). Examples of such platforms include SpiNNaker [27], Neurogrid [12], TrueNorth [23], DYNAPs [44], Tianji [54], Loihi [20], and ODIN [26], among others [52].

To cope with the growing complexity of neuromorphic systems¹, challenges in integrating emerging non-volatile memory technologies, and faster time-to-market pressure, efficient design methodologies are needed [6]. We highlight the following three key concepts that are likely to address the design issues postulated above.

- **Platform-based Design:** In this design methodology, a hardware platform is abstracted from its system software using the Application Programming Interface (API), making the hardware and software development orthogonal to allow more

Permission to make digital or hard copies of all or part of this work for personal or classroom use is granted without fee provided that copies are not made or distributed for profit or commercial advantage and that copies bear this notice and the full citation on the first page. Copyrights for components of this work owned by others than ACM must be honored. Abstracting with credit is permitted. To copy otherwise, or republish, to post on servers or to redistribute to lists, requires prior specific permission and/or a fee. Request permissions from permissions@acm.org.

ICONS '21, July 27–29, 2021, Virtual Conference

© 2021 Association for Computing Machinery.

ACM ISBN 978-1-4503-XXXX-X/18/06...\$15.00

<https://doi.org/10.1145/1122445.1122456>

¹The complexity of a neuromorphic system can be expressed in terms of the number of neurons and synapses, and their interconnection.

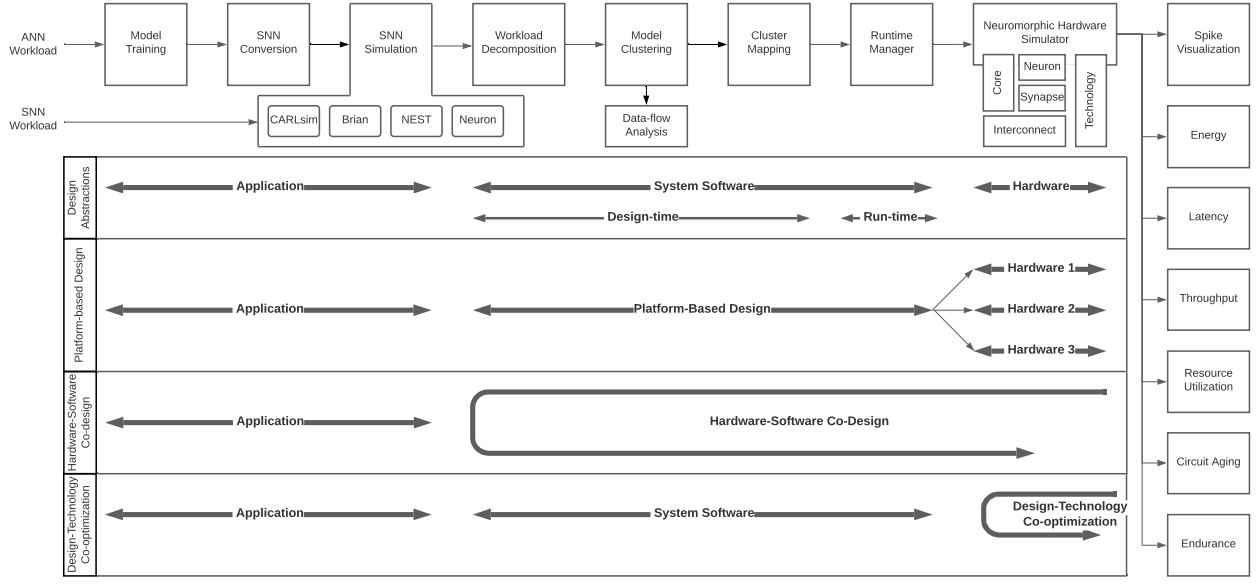


Figure 1: High-level overview of NeuroXplorer. The framework supports the following functionalities: 1) application quality exploration, 2) platform-based design, 3) hardware-software co-design, and 4) design-technology co-optimization.

effective exploration of alternative solutions [35]. Platform-based design methodology facilitates the reuse of the system software for many different hardware platforms.

- **Hardware-Software Co-design:** In this design methodology, a hardware platform and its system software are concurrently designed to exploit their synergism in order to achieve system-level design objectives [22]. The system software in this case is tailored for the hardware platform.
- **Design-Technology Co-optimization:** In this design methodology, system-level design metrics are applied to explore the choices in hardware design and process technology to enable scaling at advanced technology nodes [72].

Consequently, there is a growing need for an extensible hardware simulator and an application mapper that can perform architectural explorations with SNNs, including platform-based design, hardware-software co-design, and design-technology co-optimization. We present **NeuroXplorer**, a fast and extensible framework that is based on a *generalized template* for modeling a neuromorphic architecture that can be infused with the specific details of a given hardware and/or technology.

NeuroXplorer is released under the permissive MIT open license and it provides a user with the following high-level functionalities, which we will elaborate in the following sections.

- A design optimization engine that can incorporate hardware design metrics such as energy, latency, throughput, and reliability, as well as SNN-oriented metrics such as inter-spike interval distortion and spike disorder.
- A generalized and optimized system software framework, facilitating mapping of SNN-based applications to different neuromorphic hardware platforms.
- A cycle-accurate model of neuromorphic hardware utilizing a generalized template, which can be configured with hardware-

and technology-specific details from industrial and academic manufacturers of neuromorphic systems.

- A design space exploration framework using data flow abstractions to represent machine learning models for execution on neuromorphic hardware, allowing estimation of key system-level performance metrics early in the system design stage.
- A framework to analyze different technological alternatives for neuron and synapse circuits, and the impact of scaling in neuromorphic hardware, facilitating optimization of key system-level design metrics.

In addition to these architecture-centric functionalities, NeuroXplorer also facilitates functional simulations via SNN simulators such as CARLsim [15], Brian [29], NEST [25], and Neuron [32], supporting different degrees of neuro-biological details and learning modalities. Thus, NeuroXplorer allows to explore the design-space of application performance alongside architecture development.

NeuroXplorer is developed over a period of five years and is supported by three National Science Foundation research grants and one Department of Energy grant from the United States, and one Horizon 2020 research grant from Europe.

2 NEUROXPLOER: HIGH-LEVEL DESIGN

Figure 1 illustrates the key components of NeuroXplorer. At a high-level, NeuroXplorer supports three layers of abstraction – the **application** layer, the **system software** layer, and the **hardware** layer, similar to the abstractions in a classical von-Neumann computing system. Internally, the system software layer is divided into a **design-time** or **compile-time** methodology, where a machine learning model is converted into an intermediate form for mapping to a specific neuromorphic hardware, and a **run-time** methodology, which allocates hardware resources to admit and execute the model on the hardware. NeuroXplorer can work with both Artificial

Neural Networks (ANNs) and biology-inspired Spiking Neural Networks (SNNs). NeuroXplorer interfaces with ANN workloads that are specified in high-level frameworks such as Keras with TensorFlow backend [1, 30] and PyTorch [48]. To map an ANN workload to an event-driven neuromorphic hardware, the workload is first converted to an SNN using the **SNN Conversion** unit and then, the SNN is simulated using the **SNN Simulation** unit of NeuroXplorer.

SNN workloads can be specified in PyNN [21], which is a Python interface to many SNN simulators such as CARLsim [15], Brian [29], NEST [25], and Neuron [32]. These simulators model neural functions at various levels of detail and therefore have different requirements for computational resources. User can also specify an SNN model directly using these simulators. NeuroXplorer allows exploration of application quality using these simulators.

NeuroXplorer incorporates the spike timing information obtained from simulating an SNN model with representative training data. Such information is used to map the model to the neuromorphic hardware using the system-software framework, which consists of **Workload Decomposition**, **Model Clustering**, **Cluster Mapping**, and **Runtime Management** units.

Without loss of generality, we describe NeuroXplorer where ANN workloads are specified using Keras and SNN workloads using a combination of PyNN and PyCARL [8], a Python wrapper for SNN simulations using CARLsim. Additionally, we use our previously proposed SNN converter [4] for SNN conversion of ANN workloads in order to map them to hardware. NeuroXplorer can be trivially **extended** to work with other SNN simulation tools such as GeNN [71] and Spyketch [46], and with other SNN conversion approaches such as [43, 50, 51].

Figure 1 illustrates the three design methodologies supported by NeuroXplorer – 1) platform-based design, 2) hardware-software co-design, and 3) design-technology co-optimization. We have used NeuroXplorer to optimize for system-level design metrics, including energy [9, 19, 67], latency [3, 17], throughput [59], resource utilization [2, 11], circuit aging [5, 37, 57, 61], and endurance [65, 66, 68].

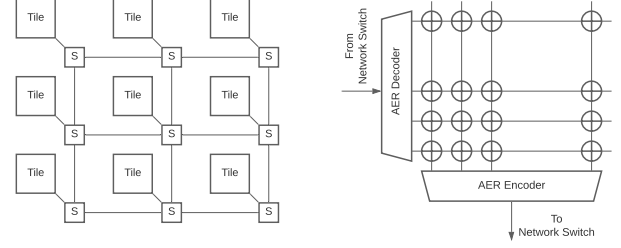
3 DETAILED DESIGN OF SYSTEM SOFTWARE

We now detail the system software of NeuroXplorer.

3.1 Platform Description

We consider a tile-based neuromorphic hardware as shown in Figure 2a. Each tile consists of a neuromorphic core, which can accommodate a certain number of neurons and synapses. A common approach to implementing a neuromorphic core is one where the synaptic cells are organized in a two-dimensional grid, known as crossbar. We illustrate a crossbar in Figure 2b.²

Typically, system designers limit the size of a crossbar to reduce energy consumption³ and mitigate the high parasitic voltage drops within a crossbar (see Figure 12). Therefore, a large machine learning model must be partitioned into *local synapses*, those that map within the crossbar of a tile, and *global synapses*, those that map



(a) A tile-based neuromorphic hardware [14]. A tile communicates spikes via the network switches (S) using a shared interconnect such as Networks-on-chip (NoC) [38] and Segmented Bus [7].

(b) A crossbar architecture. Spikes are encoded into Address Event Representation (AER). A crossbar peripheral circuitry consists of AER encoder and decoder.

Figure 2: A running example of a tile-based neuromorphic hardware. Each tile contains a neuromorphic core, which in its simplest form can be a crossbar.

on the shared interconnect [19]. To effectively address this partitioning, NeuroXplorer’s system software performs the following four key functionalities to map a machine learning workload to the hardware: workload decomposition, model clustering, cluster mapping, and runtime. We now describe these functions.

3.2 Workload Decomposition

We note that each $N \times N$ crossbar in a tile can accommodate up to N pre-synaptic connections per post-synaptic neuron, with typical value of N set between 128 (in DYNAPs) and 256 (in TrueNorth). Figure 3 illustrates an example of mapping a) one 4-input, b) one 3-input, and c) two 2-input neurons on a 4×4 crossbar. Unfortunately, neurons with more than 4 pre-synaptic connections per post-synaptic neuron cannot be mapped to this crossbar.

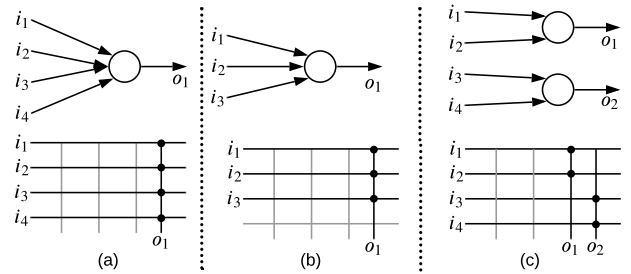


Figure 3: Example mapping of a) one 4-input, b) one 3-input, and c) two 2-input neurons to a 4×4 crossbar.

We take the example architecture of DYNAPs, where each crossbar can accommodate a maximum of 128 pre-synaptic connections. In many complex machine learning models such as LeNet, AlexNet, VGG, ResNet, and DenseNet, the number of pre-synaptic connections per post-synaptic neuron is much higher than what a crossbar in DYNAPs can accommodate.

To address this resource limitation, we have previously proposed workload decomposition, which exploits the firing principle of LIF neurons, decomposing each neuron with many pre-synaptic connections into a sequence of homogeneous fanin-of-two (FIT) neural units [11]. Figure 4 illustrates the spatial decomposition using a

²Although NeuroXplorer provides a generalized template for crossbar-based neuromorphic tiles, NeuroXplorer can be easily extended to support many different types of processing elements such as [39, 49].

³Energy consumption in a crossbar scales proportional to M^2 , where M is the input/output dimension of a crossbar.

small example of a 3-input neuron shown in Figure 4(a). We consider the mapping of this neuron to 2x2 crossbars. Since each crossbar can accommodate a maximum of two pre-synaptic connections per neuron, the example 3-input neuron cannot be mapped to the crossbar directly. The most common solution is to eliminate a synaptic connection, which may lead to accuracy loss. Figure 4(b) illustrates the decomposition mechanism, where the 3-input neuron is implemented using two FIT neural units connected in sequence as shown in Figure 4(b). Each FIT unit is similar to a 2-input neuron and it exploits the leaky integrate behavior in hardware to maintain the functional equivalence between Figures 4(a) and 4(b). Finally, Figure 4(c) illustrates the mapping of the decomposed neuron utilizing two 2x2 crossbars. The functionality of the FIT neural units is implemented using the synaptic cells of the two crossbars.

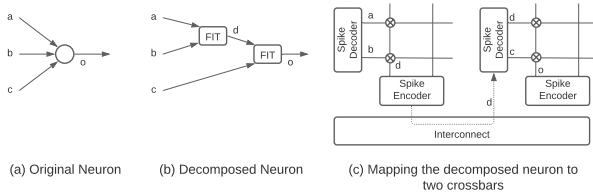


Figure 4: Illustrating the decomposition of a 3-input neuron (a) to a sequence of FIT neural units (b). The mapping of the FIT units to two 2x2 crossbars is shown in (c).

Workload decomposition is an optional function in NeuroXplorer. If this function is disabled, a machine learning model is directly fed to the clustering step. In this case, some of the pre-synaptic connections may need to be eliminated to fit onto a crossbar, which could potentially lead to accuracy loss.

3.3 Model Clustering

In the model clustering step, a large and complex machine learning model is partitioned into clusters, where each cluster consists of a fraction of the neurons and synapses of the original model that can fit onto the resources of a neuromorphic core.

Figure 5 illustrates an SNN partitioned into three clusters A, B, and C. The number of spikes communicated between a pair of neurons is indicated on its synapse. We indicate the local synapses (those that are within each cluster) in black and the global ones (those that are between clusters) in blue in this figure.

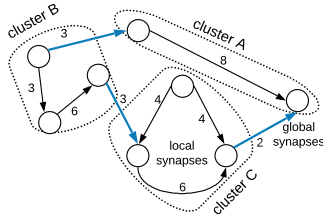
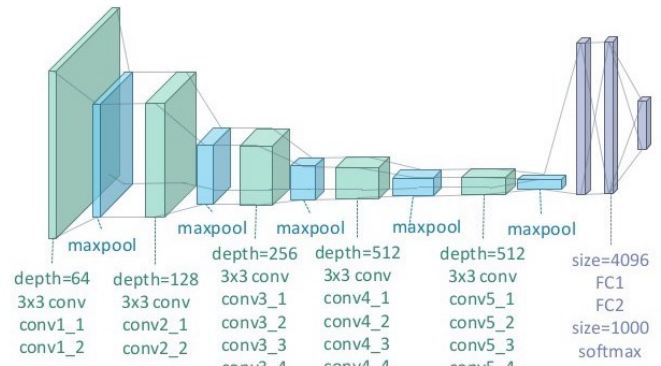


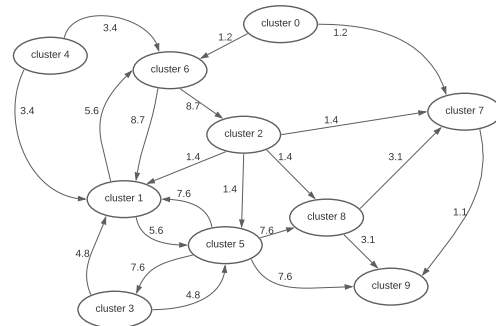
Figure 5: An SNN partitioned into three clusters.

The SNN partitioning problem is essentially a graph partitioning problem, which is NP-complete. Therefore, heuristics are typically used to find solutions. NeuroXplorer currently supports two heuristics – Particle Swarm Optimization (PSO) [33] and Kernighan-Lin

Graph Partitioning algorithm [34]. NeuroXplorer uses these heuristics to minimize 1) the number of clusters (as in [11]), which reduces the hardware requirement, and 2) the number of inter-cluster spikes (as in [9, 19]), which reduces both energy and latency when the machine learning model is mapped to hardware. NeuroXplorer can be easily extended to use other heuristics such as Hill Climbing [53] and Simulated Annealing [69], as well as other optimization objectives such as application quality and hardware reliability.



(a) VGG Convolution Neural Network (CNN).



(b) First 10 clusters of VGG generated using [9].

Figure 6: Trained VGG model and its clusters generated using model partitioning tool such as SpiNeMap [9].

Figure 6a shows the architecture of VGG for CIFAR-10 classification. Figure 6b shows the first 10 clusters generated using SpiNeMap [9].⁴ The figure illustrates the connections between these clusters, with the number on edge representing the average number of spikes communicated between the source and destination clusters when processing an image during inference. The inter-cluster links are the global synapses for mapping purposes.

3.4 Cluster Mapping

The cluster mapping step of NeuroXplorer is used to reserve computing resources of the hardware for a given machine learning model and execute the model by placing its clusters onto the physical cores. Figure 7b illustrates the placement of a clustered SNN of

⁴SpiNeMap [9] generates 95,452 clusters from the VGG model trained on CIFAR-10 dataset. For simplicity, we illustrate only the first 10 clusters and their interconnection.

Figure 7a to a neuromorphic hardware with 9 cores organized in a mesh architecture. The position of each core in the hardware is specified by a pair of Cartesian coordinates. In this example, cluster A is placed at coordinate (1,1), cluster B at (0,0), and cluster C at (2,2). All spikes between A and B, and between A and C are communicated via two interconnect segments and one hop, while all spikes between B and C are communicated via four interconnect segments and three hops. Clearly, the latency and energy on the shared interconnect depends on the placement of the clusters on the physical cores located in the Cartesian coordinate system.

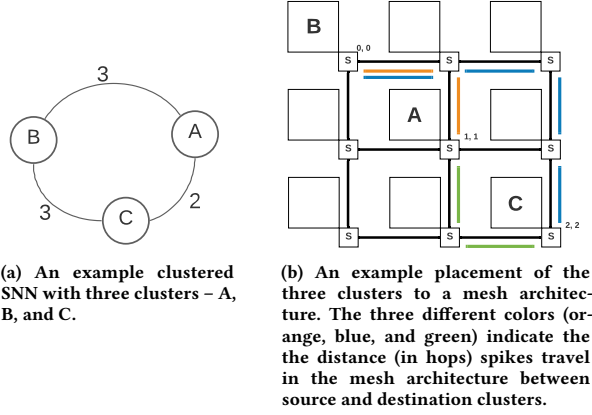


Figure 7: Example of mapping a clustered SNN on a mesh architecture.

NeuroXplorer uses an instance of PSO to optimize the placement of clusters of a machine learning model to the physical cores of the hardware, improving both latency and energy consumption. The placement solution of NeuroXplorer aims to place the clusters that communicate the most to nearby cores. NeuroXplorer can be extended to use other placement heuristics.

3.5 Runtime Manager

To illustrate the significance of a run-time manager, Figure 8 plots the spike firing rate of 100 randomly-selected neurons in AlexNet [36], a state-of-the-art CNN used for Imagenet classification. We report results for two randomly-selected training and test images.

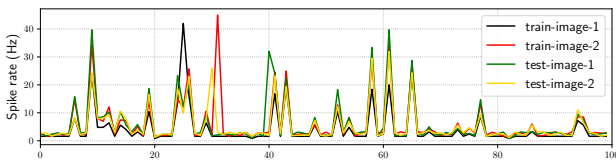


Figure 8: Spike rate of 100 randomly-selected neurons in AlexNet for 2 training images and 2 test images.

We observe that spike firing rates of neurons depend on the image presented to the AlexNet CNN. Therefore, energy and reliability improvement strategies based on design-time analysis with training examples may not be optimal when they are applied at run-time to process in-field data. Therefore, in addition to cluster placement when admitting a machine learning model to hardware,

NeuroXplorer also supports monitoring key performance statistics collected from the hardware during model execution. Such statistics can uncover bottlenecks, allowing improving system-level metrics such as energy [10] and circuit aging [5, 64] through remapping of the neurons and synapses to the hardware.

4 DETAILED DESIGN OF NEUROMORPHIC HARDWARE SIMULATOR

Figure 9 shows the high-level overview of the proposed neuromorphic hardware simulator, which facilitates cycle-accurate simulation of the interconnect and the processing tiles. Each tile models 1) a processing element, which is a neuromorphic core, 2) a router for routing spike AER packets on the shared interconnect, 3) a local memory to store cluster parameters, 4) buffer space for spike packets, and 5) AER encoder and decoder. NeuroXplorer’s hardware simulator can perform exploration with transistor technologies such as CMOS and FinFET that are used for the neurons and the peripheral circuitry in each tile, and Non-Volatile Memory (NVM) technologies such as Phase-Change Memory (PCM) [13], Oxide-Based Resistive Random Access Memory (OxRRAM) [41], Ferroelectric RAM (FeRAM) [47], and Spin-Transfer Torque Magnetic or Spin-Orbit-Torque RAM (STT/ SoT-MRAM) [70] used for synaptic weight storage.⁵ We now describe the simulator.

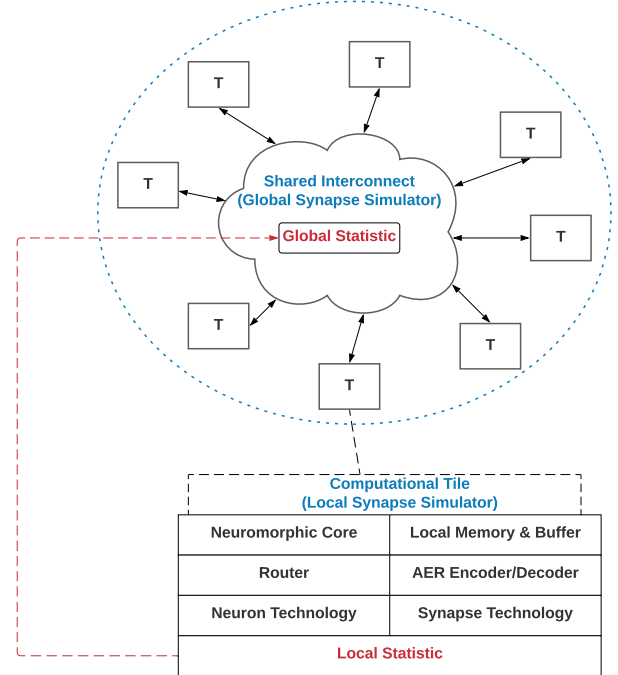


Figure 9: Architecture simulator of NeuroXplorer.

⁵Beside neuromorphic computing, NVMs are also used as main memory in conventional computers to improve performance and energy efficiency [56, 58, 60, 62, 63].

4.1 Cycle-Accurate Interconnect Simulator

Figure 10 illustrates the internal architecture of the interconnect (global synapse) simulator of NeuroXplorer in UML convention. Key components of this simulator are the following

- Spike Routing Strategy: This is the generalization class of the following routing strategies: Dyad, Negative First, North Last, Odd Even, Table-based, West-First, and XY.
- Spike Traffic Model: This is the generalization class of the following traffic models: Random, Transpose Matrix, Bit-Reversal, Butterfly, Shuffle, and Table-based.
- Configuration Manager: This is the generalization class for loading simulator parameters such as network topology, network size, traffic type, routing strategy, and simulation time.

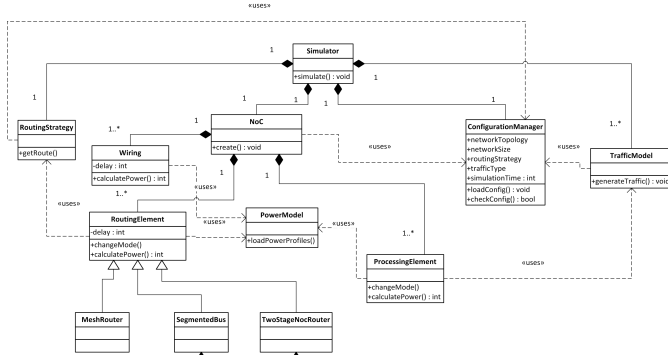


Figure 10: Class diagram of NeuroXplorer's hardware simulator using UML convention.

Figure 11 shows the capabilities of the hardware simulator of NeuroXplorer. For example, when changing the network topology, the user can select between the three interconnect types: Mesh, Segmented bus, and Two-stage NoC. The user can also input spike traffic generated from the application-level simulator at the front-end of NeuroXplorer to run hardware network simulation.

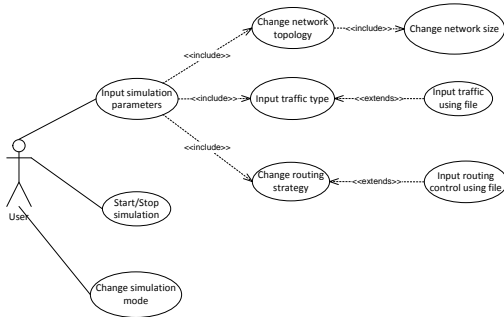


Figure 11: Use-case diagram of the hardware simulator of NeuroXplorer.

4.2 Cycle-Accurate Tile Simulator

On the computing tile front, NeuroXplorer supports detailed model of crossbars with PCM and OxRRAM-based synaptic cells. Figure 12 shows the detailed circuit model of a crossbar in NeuroXplorer with all of its parasitic components. Such parasitic components cause variable delays on the current paths inside the crossbar. For

simplicity, we have only shown the current on the shortest and the longest paths in the crossbar, where the length of a current path is measured in terms of the number of parasitic elements on the path. Therefore, spike propagation delay through synapses on longer paths is higher than on shorter paths. NeuroXplorer allows estimating these delays for a given process technology node.

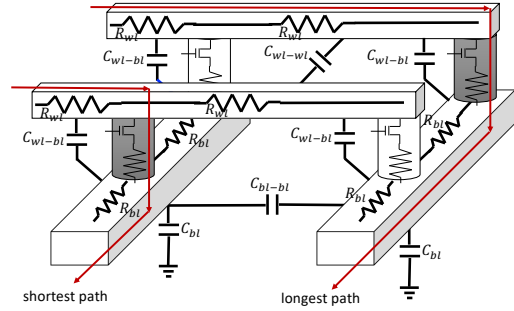


Figure 12: Detailed model of a crossbar in NeuroXplorer.

Table 1 shows the template for specifying the parasitic components in NeuroXplorer for a specific technology node.

Table 1: Generalized template for specifying the parasitic components of a crossbar in NeuroXplorer.

R_{wl}	unit wordline resistance
R_{bl}	unit bitline resistance
C_{wl}	unit wordline capacitance
C_{bl}	unit bitline capacitance
C_{wl-wl}	unit wordline to wordline capacitance
C_{wl-bl}	unit wordline to bitline capacitance
C_{bl-bl}	unit bitline to bitline capacitance

On the technology front, we briefly discuss the OxRRAM technology, as an instance of a technology that can be used for the synaptic cell. An RRAM cell is composed of an insulating film sandwiched between conducting electrodes forming a metal-insulator-metal (MIM) structure (see Figure 13). Recently, filament-based metal-oxide RRAM implemented with transition-metal-oxides such as HfO_2 , ZrO_2 , and TiO_2 has received considerable attention due to their low-power and CMOS-compatible scaling. Synaptic weights are represented as conductance of the insulating layer within each RRAM cell. To program an RRAM cell, elevated voltages are applied at the top and bottom electrodes, which re-arranges the atomic structure of the insulating layer. Figure 13 shows the High-Resistance State (HRS) and the Low-Resistance State (LRS) of an RRAM cell. In NeuroXplorer, the RRAM cell can also be programmed into intermediate low-resistance states, allowing its multilevel operations. For instance, to implement two bits per synapse we can program the RRAM cell for one HRS and three LRS states.

NeuroXplorer also supports implementing many variants of Integrate & Fire (I&F) neuron. Table 2 provides the template for specifying the parameters for a neuron and synaptic cell in a crossbar.

The generalized template of Tables 1 and 2 can be infused with the specific details of a present-day neuromorphic chip and evaluate the impact of technology scaling on system-level metrics such as energy, latency, and reliability. We now present the evaluation of NeuroXplorer by configuring it with the parameters of the DYNAPs

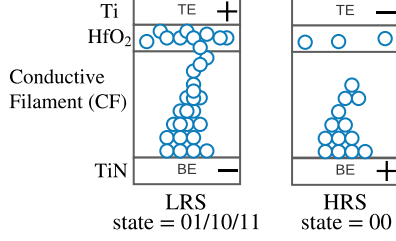


Figure 13: Operation of an RRAM cell with the HfO₂ layer sandwiched between the metals Ti (top electrode) and TiN (bottom electrode). The left subfigure shows the formation of LRS states with the formation of conducting filament (CF). This represents logic states 01, 10, and 11. The right subfigure shows the depletion of CF on application of a negative voltage on the TE. This represents the HRS state or logic 00.

Table 2: Generalized template for specifying the parameters of a neuron and synaptic cell in NeuroXplorer.

Neuron technology	CMOS or FinFET
Technology node	65nm, 45nm, 32nm, and 16nm
Supply voltage	1.0V
Energy per spike	50pJ at 30Hz spike frequency
Synapse technology	OxRRAM or PCM
Access device	Diode or FET or NMOS
Resistance states	1-bit/synapse or 2-bit/synapse

neuromorphic hardware [44] at 45nm node with 2-bit synapses implemented using OxRRAM-based 1T1R cells.

5 EVALUATION OF NEUROXPLORER

Recently, SNNs are used to improve the quality of machine learning applications [16, 31, 45, 55]. We select 10 machine learning programs which are representative of three most commonly-used neural network classes: convolutional neural network (CNN), multi-layer perceptron (MLP), and recurrent neural network (RNN). Table 3 summarizes the topology, the number of neurons and synapses, the number of spikes per image, and the baseline accuracy of these applications on the DYNAPs neuromorphic hardware.

Table 3: Applications used to evaluate NeuroXplorer.

Class	Applications	Dataset	Neurons	Synapses	Avg. Spikes/Frame	Accuracy
CNN	LeNet	MNIST	23,687	275,110	724,565	85.1%
	DenseNet	CIFAR-10	17,450	198,470	1,250,976	42.8%
	AlexNet	ImageNet	259,604	3,873,222	7,055,109	69.8%
	ResNet	CIFAR-10	267,488	35,391,616	7,339,322	57.4%
	VGG	ImageNet	623,635	12,215,209	12,826,673	90.7%
	HeartClass [18]	Physionet	170,292	1,049,249	2,771,634	63.7%
MLP	MLPDigit	MNIST	894	79,400	26,563	91.6%
	EdgeDet [15]	CARLsim	7,268	114,057	248,603	100%
	ImgSmooth [15]	CARLsim	5,120	9,025	174,872	100%
RNN	RNNDigit [24]	MNIST	1,191	11,442	30,508	83.6%

We evaluate the following three configurations of NeuroXplorer.

- **PyCARL** [8]: This is our default configuration, where a machine learning model is clustered arbitrarily. Clusters are also mapped arbitrarily to the crossbars of a hardware.
- **SpiNeMap** [9]: In this configuration, NeuroXplorer clusters a machine learning model to minimize the inter-cluster spike communication. Clusters are mapped to the crossbars to reduce energy consumption on the shared interconnect.

- **DecomposedSNN** [11]: In this configuration, NeuroXplorer decomposes a machine learning model to pack its neurons and synapses densely into each crossbar. The clusters are mapped to the crossbars to reduce spike latency and energy consumption on the shared interconnect.

5.1 Software Exploration: Cluster Count

Figure 14 plots the cluster count for each evaluated application for three different configurations of NeuroXplorer, normalized to PyCARL. For reference, the number of clusters obtained using PyCARL is indicated for each application. We observe that different configurations of NeuroXplorer lead to different cluster counts. DecomposedSNN, which maximizes the neuron and synapse utilization within each cluster, generates the lowest cluster count (44.5% lower than PyCARL and 50.1% lower than SpiNeMap).

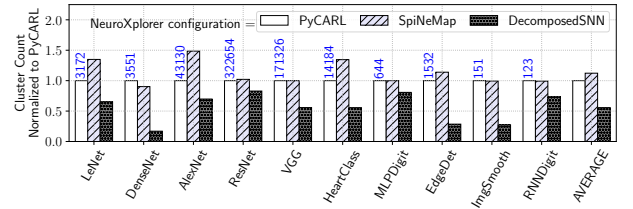


Figure 14: Cluster count using NeuroXplorer.

5.2 Software Exploration: Spike Count

Figure 15 plots the total number of spikes on the shared interconnect (called global spikes) for each evaluated application for three different configurations of NeuroXplorer, normalized to PyCARL. We observe that SpiNeMap has the lowest number of global spikes (6% lower than PyCARL and 34% lower than DecomposedSNN), which reduces both spike latency and communication energy due to reduction of the congestion on the interconnect.

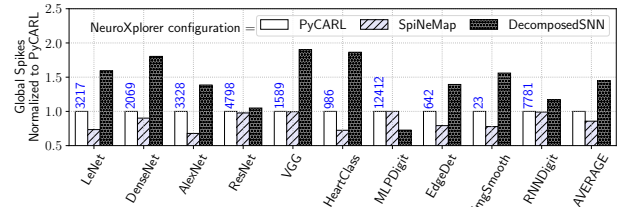


Figure 15: Global spikes using NeuroXplorer.

5.3 Hardware Exploration: Energy and ISI

Figure 16 and 17 plot respectively, the communication energy and inter-spike interval (ISI) of each evaluated application using four NoC routing techniques of NeuroXplorer normalized to XY routing. For reference, the communication energy and ISI at 45nm technology node with XY routing is also indicated.

5.4 Technology Exploration: Inference Lifetime

Non-Volatile Memories (NVMs) suffer from read endurance problem, where an NVM cell can switch its state upon repeated access. Therefore, the programmed synaptic weights of the NVM cells in a

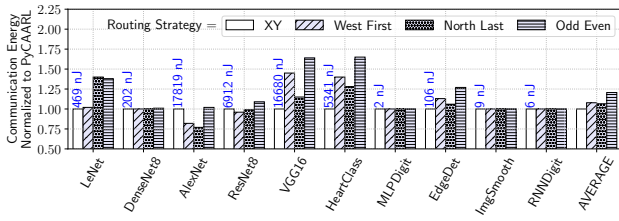


Figure 16: Communication energy using NeuroXplorer.

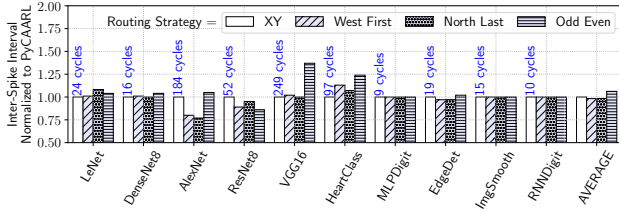


Figure 17: Inter-spike interval (ISI) using NeuroXplorer.

neuromorphic hardware needs to be reprogrammed periodically. To this end, inference lifetime refers to how many images can be successfully inferred using the hardware before reprogramming of the synaptic weights becomes necessary. Figure 18 plots the impact of technology scaling on the inference lifetime of a neuromorphic hardware. At scaled nodes, the read endurance of NVMs reduces, which lowers the inference lifetime.

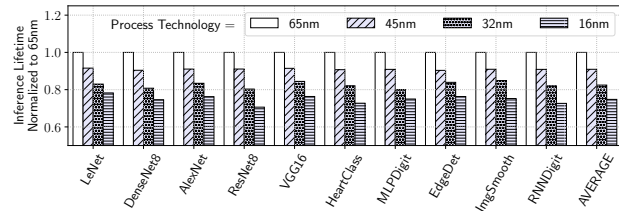


Figure 18: Technology exploration using NeuroXplorer.

6 CONCLUSIONS

We propose NeuroXplorer, an extensible framework for architectural exploration with Spiking Neural Networks (SNN). NeuroXplorer is based on a generalized template and can be infused with specific details of a neuromorphic hardware and technology. NeuroXplorer can perform platform-based design, hardware-software co-design, and design-technology co-optimization, enabling system designers to explore a variety of both application as well as platform design configurations to meet the needs of emerging workloads as well as newer design technologies. In addition to these architecture-centric functionalities, NeuroXplorer also facilitates functional simulations via SNN simulators supporting different degrees of neuro-biological details and learning modalities, allowing exploration of application quality.

REFERENCES

- [1] M. Abadi et al., "Tensorflow: A system for large-scale machine learning," in *OSDI*, 2016.
- [2] A. Balaji et al., "Compiling spiking neural networks to mitigate neuromorphic hardware constraints," in *IGSC Workshops*, 2020.

- [3] A. Balaji et al., "A framework for the analysis of throughput-constraints of SNNs on neuromorphic hardware," in *ISVLSI*, 2019.
- [4] A. Balaji et al., "Power-accuracy trade-offs for heartbeat classification on neural networks hardware," *JOLPE*, 2018.
- [5] A. Balaji et al., "A framework to explore workload-specific performance and lifetime trade-offs in neuromorphic computing," *CAL*, 2019.
- [6] A. Balaji et al., "Design methodology for embedded approximate artificial neural networks," in *GLSVLSI*, 2019.
- [7] A. Balaji et al., "Exploration of segmented bus as scalable global interconnect for neuromorphic computing," in *GLSVLSI*, 2019.
- [8] A. Balaji et al., "PyCARTL: A PyNN interface for hardware-software co-simulation of spiking neural network," in *IJCNN*, 2020.
- [9] A. Balaji et al., "Mapping spiking neural networks to neuromorphic hardware," *TVLSI*, 2020.
- [10] A. Balaji et al., "Run-time mapping of spiking neural networks to neuromorphic hardware," *JSPS*, 2020.
- [11] A. Balaji et al., "Enabling resource-aware mapping of spiking neural networks via spatial decomposition," *ESL*, 2020.
- [12] B. V. Benjamin et al., "Neurogrid: A mixed-analog-digital multichip system for large-scale neural simulations," *Proceedings of the IEEE*, 2014.
- [13] G. W. Burr et al., "Neuromorphic computing using non-volatile memory," *Advances in Physics: X*, 2017.
- [14] F. Catthoor et al., "Very large-scale neuromorphic systems for biological signal processing," in *CMOS Circuits for Biological Sensing and Processing*, 2018.
- [15] T. Chou et al., "CARLsim 4: An open source library for large scale, biologically detailed spiking neural network simulation using heterogeneous clusters," in *IJCNN*, 2018.
- [16] A. Das et al., "Unsupervised heart-rate estimation in wearables with Liquid states and a probabilistic readout," *Neural Networks*, 2018.
- [17] A. Das et al., "Dataflow-based mapping of spiking neural networks on neuromorphic hardware," in *GLSVLSI*, 2018.
- [18] A. Das et al., "Heartbeat classification in wearables using multi-layer perceptron and time-frequency joint distribution of ECG," in *CHASE*, 2018.
- [19] A. Das et al., "Mapping of local and global synapses on spiking neuromorphic hardware," in *DATE*, 2018.
- [20] M. Davies et al., "Loihi: A neuromorphic manycore processor with on-chip learning," *IEEE Micro*, 2018.
- [21] A. P. Davison et al., "PyNN: a common interface for neuronal network simulators," *Frontiers in Neuroinformatics*, 2009.
- [22] G. De Michell et al., "Hardware/software co-design," *Proceedings of the IEEE*, 1997.
- [23] M. V. Debole et al., "TrueNorth: Accelerating from zero to 64 million neurons in 10 years," *Computer*, 2019.
- [24] P. Diehl et al., "Unsupervised learning of digit recognition using spike-timing-dependent plasticity," *Front. in Comp. Neuroscience*, 2015.
- [25] J. M. Eppler et al., "Pynest: a convenient interface to the nest simulator," *Frontiers in Neuroinformatics*, 2009.
- [26] C. Frenkel et al., "A 0.086-mm² 12.7-pj/sop 64k-synapse 256-neuron online-learning digital spiking neuromorphic processor in 28-nm CMOS," *TBCAS*, 2018.
- [27] S. B. Furber et al., "The SpiNNaker project," *Proceedings of the IEEE*, 2014.
- [28] S. Fusi et al., "Collective behavior of networks with linear (vlsi) integrate-and-fire neurons," *Neural Computation*, 1999.
- [29] D. F. Goodman et al., "The brian simulator," *Frontiers in Neuroscience*, 2009.
- [30] A. Gulli et al., *Deep learning with Keras*, 2017.
- [31] K. Hamilton et al., "Modeling epidemic spread with spike-based models," in *ICONS*, 2020.
- [32] M. L. Hines et al., "The NEURON simulation environment," *Neural Computation*, 1997.
- [33] J. Kennedy et al., "Particle swarm optimization," in *ICNN*, 1995.
- [34] B. W. Kernighan et al., "An efficient heuristic procedure for partitioning graphs," *Bell System Technical Journal*, 1970.
- [35] K. Keutzer et al., "System-level design: Orthogonalization of concerns and platform-based design," *TCAD*, 2000.
- [36] A. Krizhevsky et al., "Imagenet classification with deep convolutional neural networks," in *Advances in neural information processing systems (NeurIPS)*, 2012.
- [37] S. Kundu et al., "Special session: Reliability analysis for ML/AI hardware," in *VTS*, 2021.
- [38] X. Liu et al., "Neu-NoC: A high-efficient interconnection network for accelerated neuromorphic systems," in *ASP-DAC*, 2018.
- [39] D. Ma et al., "Darwin: A neuromorphic hardware co-processor based on spiking neural networks," *JSA*, 2017.
- [40] W. Maass, "Networks of spiking neurons: The third generation of neural network models," *Neural Networks*, 1997.
- [41] A. Mallik et al., "Design-technology co-optimization for oxrram-based synaptic processing unit," in *VLSIT*, 2017.
- [42] C. Mead, "Neuromorphic electronic systems," *Proc. of the IEEE*, 1990.
- [43] R. Midya et al., "Artificial neural network (ANN) to spiking neural network (SNN) converters based on diffusive memristors," *Advanced Electronic Materials*, 2019.

- [44] S. Moradi *et al.*, “A scalable multicore architecture with heterogeneous memory structures for dynamic neuromorphic asynchronous processors (DYNAPs),” *TBCAS*, 2017.
- [45] E. J. Moyer *et al.*, “Machine learning applications to DNA subsequence and restriction site analysis,” in *SPMB*, 2020.
- [46] M. Mozafari *et al.*, “Spyketorch: Efficient simulation of convolutional spiking neural networks with at most one spike per neuron,” *Frontiers in Neuroscience*, 2019.
- [47] H. Mulaosmanovic *et al.*, “Novel ferroelectric FET based synapse for neuromorphic systems,” in *VLSIT*, 2017.
- [48] A. Paszke *et al.*, “PyTorch: An imperative style, high-performance deep learning library,” *arXiv*, 2019.
- [49] N. Qiao *et al.*, “A reconfigurable on-line learning spiking neuromorphic processor comprising 256 neurons and 128k synapses,” *Frontiers in Neuroscience*, 2015.
- [50] B. Rueckauer *et al.*, “Conversion of analog to spiking neural networks using sparse temporal coding,” in *ISCAS*, 2018.
- [51] B. Rueckauer *et al.*, “Theory and tools for the conversion of analog to spiking convolutional neural networks,” *arXiv*, 2016.
- [52] C. D. Schuman *et al.*, “A survey of neuromorphic computing and neural networks in hardware,” *arXiv preprint arXiv:1705.06963*, 2017.
- [53] B. Selman *et al.*, “Hill-climbing search,” *En. of Cog. Sc.*, 2006.
- [54] L. Shi *et al.*, “Development of a neuromorphic computing system,” in *IEDM*, 2015.
- [55] J. D. Smith *et al.*, “Solving a steady-state PDE using spiking networks and neuromorphic hardware,” in *ICONS*, 2020.
- [56] S. Song *et al.*, “Design methodologies for reliable and energy-efficient PCM systems,” in *IGSC Workshops*, 2020.
- [57] S. Song *et al.*, “A case for lifetime reliability-aware neuromorphic computing,” in *MWSCAS*, 2020.
- [58] S. Song *et al.*, “Enabling and exploiting partition-level parallelism (PALP) in phase change memories,” *TECS*, 2019.
- [59] S. Song *et al.*, “Compiling spiking neural networks to neuromorphic hardware,” in *LCTES*, 2020.
- [60] S. Song *et al.*, “Exploiting inter- and intra-memory asymmetries for data mapping in hybrid tiered-memories,” in *ISMM*, 2020.
- [61] S. Song *et al.*, “Improving dependability of neuromorphic computing with non-volatile memory,” in *EDCC*, 2020.
- [62] S. Song *et al.*, “Improving phase change memory performance with data content aware access,” in *ISMM*, 2020.
- [63] S. Song *et al.*, “Aging-aware request scheduling for non-volatile main memory,” in *ASP-DAC*, 2021.
- [64] S. Song *et al.*, “Dynamic reliability management in neuromorphic computing,” *JETC*, 2021.
- [65] T. Titirsha *et al.*, “Reliability-performance trade-offs in neuromorphic computing,” in *IGSC Workshops*, 2020.
- [66] T. Titirsha *et al.*, “Thermal-aware compilation of spiking neural networks to neuromorphic hardware,” in *LCPC*, 2020.
- [67] T. Titirsha *et al.*, “On the role of system software in energy management of neuromorphic computing,” in *CF*, 2021.
- [68] T. Titirsha *et al.*, “Endurance-aware mapping of spiking neural networks to neuromorphic hardware,” *TPDS*, 2021.
- [69] P. J. Van Laarhoven *et al.*, “Simulated annealing,” in *Simulated annealing: Theory and applications*, 1987.
- [70] A. F. Vincent *et al.*, “Spin-transfer torque magnetic memory as a stochastic memristive synapse for neuromorphic systems,” *TBCAS*, 2015.
- [71] E. Yavuz *et al.*, “GeNN: a code generation framework for accelerated brain simulations,” *Scientific Reports*, 2016.
- [72] G. Yeric *et al.*, “The past present and future of design-technology co-optimization,” in *CICC*, 2013.